February 9, 2008

# Triaxial projected shell model approach

J.A. Sheikh[1,2,3] and K. Hara[1]

[1] *Physik-Department, Technische Universität München, D-85747 Garching, Germany*

[2] *Institut de Recherches Subatomiques (IReS), Universite Louis Pasteur, 23 rue du Loess, F-67037 Strasbourg Cedex 2, France*

[3] *Tata Institute of Fundamental Research, Colaba, Bombay - 400 005, India*

## Abstract

The projected shell model analysis is carried out using the triaxial Nilsson+BCS basis. It is demonstrated that, for an accurate description of the moments of inertia in the transitional region, it is necessary to take the triaxiality into account and perform the three-dimensional angular-momentum projection from the triaxial Nilsson+BCS intrinsic wavefunction.

PACS numbers : 21.60.Cs, 21.10.Hw, 21.10.Ky, 27.50.+e

The major advancement in the studies of deformed nuclei has been the introduction of the Nilsson potential [1]. It was shown that the rotational properties of deformed nuclei can be described by considering nucleons to move in a deformed potential. The description of the deformed nuclei in medium and heavy mass regions is impossible using the standard (spherical) shell model approach, despite the recent progress in the computing power. The Nilsson model has provided a useful nomenclature for the observed rotational bands. It is known that each rotational band is built on an intrinsic Nilsson state. The Nilsson or deformed state is defined in the intrinsic frame of reference in which the rotational symmetry has been broken and in order to calculate the observable properties, it is required to restore the broken symmetry.

The rotational symmetry can be restored by using the standard angular momentum projection operator [2]. This method has been used to project out the good angular momentum states from the Nilsson+BCS intrinsic state [3–5], see also the review article [6] and references cited therein. In this approach, the angular momentum projection is carried out from a chosen set of Nilsson+BCS states near the Fermi-surface. The projected states are then used to diagonalize a shell model Hamiltonian. This approach referred to as the projected shell model (PSM) follows the basic philosophy of the standard shell model approach. The only difference is that, in the PSM, the deformed basis is employed rather than the spherical basis. This makes the truncation of the many-body basis very efficient, so that the shell model calculations even for heavier systems can be easily performed.

The PSM approach has been used to describe a broad range of nuclear phenomena such as backbending [7], superdeformed [8,9] and identical bands [10] with considerable success. The assumption in the PSM approach has been the axial symmetry for the deformed system to keep the computation simple. In fact, this is a reasonable approximation for well deformed nuclei. However, for transitional nuclei, this assumption is questionable. The inadequacy of the axially symmetric basis has been clearly demonstrated by moments of inertia (the backbending plots) of the transitional nuclei in the rare-earth region. It has been shown [6] that, in the low spin region, observed moments of inertia for lighter rare-earth nuclei (for instance $^{156}$Er, $^{158}$Er, $^{158}$Yb and $^{162}$Hf) and for the heavier rare-earth nuclei (for instance $^{172}$W, $^{174}$W and $^{176}$W) increase quite steeply with increasing rotational frequency as compared to the moment of inertia calculated by the axially symmetric PSM approach (see Figs. 14–17 in [6]). This can be understood by noting that the horizontal (vertical) line in the backbending plot represents the rotational (vibrational) limit since the energy $E(I)$ as a function of spin $I$ is proportional to $I^2$ ($I$). In this sense, the experimental data slants towards the vibrational side in comparison with the existing PSM results. On the other hand, the spectrum of a triaxial rotor [11] is known to vary from rotational spectrum to a vibrational one as the triaxiality parameter $\gamma$ increases from 0 to $30^o$ and, using this model, it has been demonstrated (see Fig. 18 in [6]) that the backbending plot indeed slants towards the vibrational limit when $\gamma$ increases. It is therefore expected that, by using the triaxial basis in the PSM, the moments of inertia and other properties of the transitional nuclei can be described more appropriately. As pointed out in [6], the major problem here lies rather in the ground state band. This part of the spectrum is quite insensitive to the configuration mixing since the energy and spin values are still low ($I \leq 10$), so that an improvement of the ground state by allowing some triaxiality is in order. The purpose of the present work is to develop a triaxial projected shell model (referred to as TPSM hereafter)

approach for the description of transitional nuclei. This requires a three-dimensional angular momentum projection and has not been attempted so far except for a short investigation in early eighties [12]. We have carried out the three-dimensional projection and would like to report our preliminary results.

The shell model Hamiltonian employed is identical to the one used in the axially symmetric PSM approach [6]. It consists of $Q \cdot Q$ + monopole pairing + quadrupole pairing forces

$$\hat{H} = \hat{H}_0 - \frac{\chi}{2} \sum_{\mu} \hat{Q}^{\dagger}_{\mu} \hat{Q}_{\mu} - G_M \hat{P}^{\dagger} \hat{P} - G_Q \sum_{\mu} \hat{P}^{\dagger}_{\mu} \hat{P}_{\mu}. \tag{1}$$

Here, $\hat{H}_0$ is the the spherical harmonic-oscillator single-particle Hamiltonian with a proper $l \cdot s$-force while the operators $\hat{Q}$ and $\hat{P}$ are defined as

$$\hat{Q}_{\mu} = \sum_{\alpha\beta} Q_{\mu\alpha\beta} c^{\dagger}_{\alpha} c_{\beta}, \quad \hat{P}^{\dagger} = \frac{1}{2} \sum_{\alpha} c^{\dagger}_{\alpha} c^{\dagger}_{\bar{\alpha}}, \quad \hat{P}^{\dagger}_{\mu} = \frac{1}{2} \sum_{\alpha\beta} Q_{\mu\alpha\beta} c^{\dagger}_{\alpha} c^{\dagger}_{\bar{\beta}}, \tag{2}$$

where the quadrupole matrix-elements are given by

$$Q_{\mu\alpha\alpha'} = \delta_{NN'} (Njm|Q_{\mu}|N'j'm'). \tag{3}$$

In Eq. (2), $\alpha = \{Njm\}$ while $\bar{\alpha}$ represents the time-reversed state of $\alpha$. The Hartree-Fock-Bogoliubov (HFB) approximation of the shell model Hamiltonian Eq. (1) leads to the quadrupole mean-field which is similar to the Nilsson potential. Therefore, instead of performing the HFB variational analysis of the Hamiltonian in Eq. (1), the Nilsson potential can be directly used to obtain the deformed basis. In the present work, we use the triaxial Nilsson potential specified by the deformation parameters $\epsilon$ and $\epsilon'$

$$\hat{H}_N = \hat{H}_0 - \frac{2}{3} \hbar\omega (\epsilon \hat{Q}_0 + \epsilon' \frac{\hat{Q}_{+2} + \hat{Q}_{-2}}{\sqrt{2}}), \tag{4}$$

to generate the deformed single-particle wavefunctions. It can be easily seen that the rotation operator $e^{-\imath \frac{\pi}{2} \hat{J}_z}$ transforms the Nilsson Hamiltonian $\hat{H}_N$ into the opposite triaxiality ($\epsilon' \rightarrow -\epsilon'$) leaving the eigenvalues unchanged. Later, it will be shown that the projected energy is independent of the sign of $\epsilon'$ and it is sufficient to consider only the non-negative $\epsilon'$. The volume conservation also restricts the range of $\epsilon$ and $\epsilon'$ values to

$$-3 < \epsilon < \frac{3}{2}, \quad |\epsilon'| < \sqrt{3}(1 + \frac{\epsilon}{3}). \tag{5}$$

The triaxial Nilsson potential has been solved for the rare-earth region with three major shells $N = 4, 5, 6$ $(3, 4, 5)$ for neutrons (protons).

In the next step, the monopole pairing Hamiltonian is treated based on the triaxial Nilsson basis. We use the standard strengths for the pairing interaction of the form

$$G_M = (G_1 \mp G_2 \frac{N - Z}{A}) \frac{1}{A}, \tag{6}$$

where $-$ $(+)$ is for neutrons (protons) while $G_1$ and $G_2$ are chosen respectively as 21.24 and 13.86 MeV in the rare-earth region. The pairing correlations are treated by using the usual

BCS approximation to establish the Nilsson+BCS basis. The three-dimensional angular momentum projection is then carried out on the quasiparticle states obtained in this way.

The three-dimensional angular momentum projection operator is given by

$$\hat{P}^I_{MK} = \frac{2I+1}{16\pi^2} \int d\Omega D^I_{MK}(\Omega) \hat{R}(\Omega), \tag{7}$$

$\hat{R}(\Omega) = e^{-\imath\alpha\hat{J}_z} e^{-\imath\beta\hat{J}_y} e^{-\imath\gamma\hat{J}_z}$ being the rotation operator and $D^I_{MK}(\Omega) =< \nu IM|\hat{R}(\Omega)|\nu IK >^*$ its irreducible representation where $\{|\nu IM >\}$ is a complete set of states for the specified angular momentum quantum number $IM$. Since the spectral representation of the projection operator Eq. (7) is represented by

$$\hat{P}^I_{MK} = \sum_\nu |\nu IM >< \nu IK|, \tag{8}$$

it is easy to see that $|\Phi' >\equiv e^{-\imath\frac{\pi}{2}\hat{J}_z}|\Phi >$, i.e. the state of the opposite triaxiality to a state $|\Phi >$, is projected to give

$$\hat{P}^I_{MK}|\Phi' >= \hat{P}^I_{MK} e^{-\imath\frac{\pi}{2}\hat{J}_z}|\Phi >= (-)^{-\imath\frac{\pi}{2}K} \hat{P}^I_{MK}|\Phi > . \tag{9}$$

This state differs only by a phase factor from $\hat{P}^I_{MK}|\Phi >$ and thus represents the same physical state. It therefore proves that the result of the angular momentum projection should be independent of the sign of $\epsilon'$. We have used this property to check the programming since it is a non-trivial relation. Note that this justifies the above-mentioned restriction $\epsilon' \geq 0$. Details of the projection technique and algorithm are discussed in an Appendix of [6].

In the present work, we have diagonalized the Hamiltonian Eq. (1) within the space spanned by $\{\hat{P}^I_{MK}|\Phi >\}$ where $|\Phi >$ is the (triaxial) quasiparticle vacuum state. The TPSM eigenvalue equation with the eigenvalue $E^I$ for a given spin $I$ thus becomes

$$\sum_{K'} \left( H^I_{KK'} - E^I N^I_{KK'} \right) F^I_{K'} = 0 \tag{10}$$

where the matrix elements are defined by

$$H^I_{KK'} =< \Phi|\hat{H}\hat{P}^I_{KK'}|\Phi >, \quad N^I_{KK'} =< \Phi|\hat{P}^I_{KK'}|\Phi > . \tag{11}$$

This TPSM equation has been solved for a range of nuclei in the rare-earth region and the results of a selected few are presented in Figs. 1 and 2.

The deformation parameters $\epsilon$ used in Fig. 1 are exactly the same as those used in the earlier calculations with the axially symmetric basis [6], i.e. $\epsilon = 0.20$, 0.20 and 0.225 for $^{156}$Er, $^{158}$Yb and $^{176}$W, respectively. The results with $\epsilon' = 0.0$ in Figs. 1 and 2 represent these axially symmetric calculations. The experimental moments of inertia (represented by circles) increase very steeply. The calculations with $\epsilon' = 0.0$ on the other hand depict a very slow increase and is typical of an axially deformed rotational band. The moments of inertia in Fig. 1 become steeper with increasing value of $\epsilon'$ and the value close to $\epsilon' = 0.15$ reproduces the experimental data. Roughly speaking, this $\epsilon'$ value corresponds to $\gamma = 35^0$. It should be noted that the experimental moment of inertia shown in Fig. 1 slightly increases, in particular for $^{176}$W, at the higher end, whereas the theoretical moment of inertia shows

a drop. This increase in the observed moment of inertia can be explained by noting that, at around spin I=$12^+$, a 2-quasiparticle band (i.e. the s-band) will cross with the ground band and the energy of the higher spin states will be depressed, so that the moment of inertia will effectively increase. In the present calculations, the projection has been carried out only from the ground (i.e. the 0-quasiparticle) band and this effect is not taken into account. The projection from 2- and higher-quasiparticle states requires further work and will be reported elsewhere.

Fig. 2 shows the moments of inertia for some Os-isotopes. It is known that these isotopes are $\gamma$ soft with very low-lying $\gamma$ bands. It is clear from Fig. 2 that, for $^{184}$Os, the moment of inertia is well reproduced with $\epsilon' = 0.15$. For $^{186}$Os and $^{188}$Os, the experimental moment of inertia can be explained with $\epsilon'$ between 0.10 and 0.15.

In summary, it has been clearly shown in the present work that three-dimensional angular momentum projection from triaxial Nilsson+BCS deformed intrinsic wavefunction is essential for an accurate description of the transitional nuclei. The moments of inertia of these transitional nuclei depict a steep increase as a function of rotational frequency in the low spin region and this can only be explained with triaxial deformation of $\gamma \simeq 30^0$ since the inclusion of 2- and higher-quasiparticle bands will affect little in this spin region.

We would like to mention that the present work has been exploratory. For a detailed study, the energy-surface needs to be analyzed as a function of $\epsilon$ and $\epsilon'$ to look for the optimal deformation. In the present work, the deformation parameter $\epsilon$ has been taken from the earlier studies in which the axial symmetry was assumed. In a more consistent treatment, both $\epsilon$ and $\epsilon'$ have to be varied in order to search the energy minimum for spin $I = 0$ [12].

# REFERENCES


[1] S.G. Nilsson, Dan. Mat. Fys. Medd. **29**, Nr.16 (1955)

[2] P. Ring and P. Schuck, *The Nuclear Many-Body Problem*, Springer Verlag, Heidelberg, New York, 1980

[3] K.Hara and S. Iwasaki, Nucl. Phys. **332** (1979) 61

[4] K.Hara and S. Iwasaki, Nucl. Phys. **348** (1980) 200

[5] K.Hara and S. Iwasaki, Prog. Theor. Phys. **68** (1982) 1782

[6] K. Hara and Y. Sun, Int. J. Mod. Phys. **E4** Nr.4 (1995) 637

[7] K. Hara and Y. Sun, Nucl. Phys. **A529** (1990) 445

[8] Y. Sun and M. Guidry, Phys. Rev. **C52** (1995) R2844

[9] Y. Sun, J.-y. Zhang and M. Guidry, Phys. Rev. Lett. **78** (1997) 2321

[10] Y. Sun, C.-L. Wu, D.H. Feng, J.L. Egido and M. Guidry, Phys. Rev. **C53** (1996) 2227

[11] A.S. Davydov and F.G. Filippov, Nucl. Phys. **8** (1958) 237

[12] A. Hayashi, K. Hara and P. Ring, Phys. Rev. Lett. **53** (1984) 337

## FIGURES

FIG. 1. The experimental and the calculated moments of inertia ($\Theta$) are plotted as a function of the rotational frequency ($\omega$) for $^{156}$Er, $^{158}$Yb and $^{176}$W. It is very evident that the Expt. moment of inertia is reproduced with the triaxiality $\epsilon' \simeq 0.15$ for all the three cases.

FIG. 2. The experimental and the calculated moments of inertia ($\Theta$) are plotted as a function of the rotational frequency ($\omega$) for $^{184}$Os, $^{186}$Os and $^{188}$Os. For $^{184}$Os, the Expt. moment of inertia is very well reproduced with $\epsilon' \simeq 0.15$. For $^{186}$Os and $^{188}$Os, it can be described with $\epsilon'$ between 0.10 and 0.15.

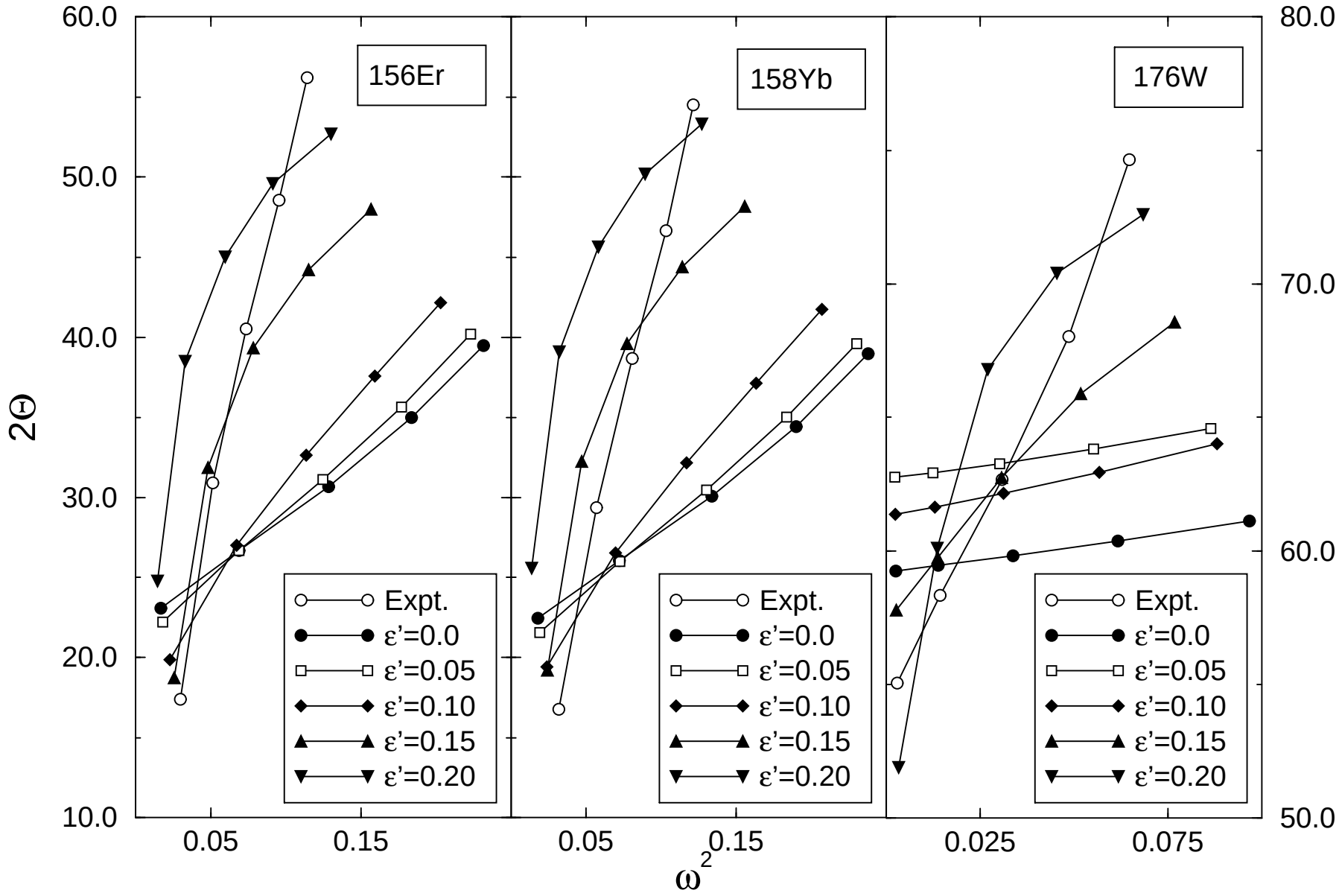
156Er
158Yb
176W
Expt.
ε'=0.0
ε'=0.05
ε'=0.10
ε'=0.15
ε'=0.20
2Θ
ω2
60.0
50.0
40.0
30.0
20.0
10.0
80.0
70.0
60.0
50.0
0.05
0.15
0.025
0.075

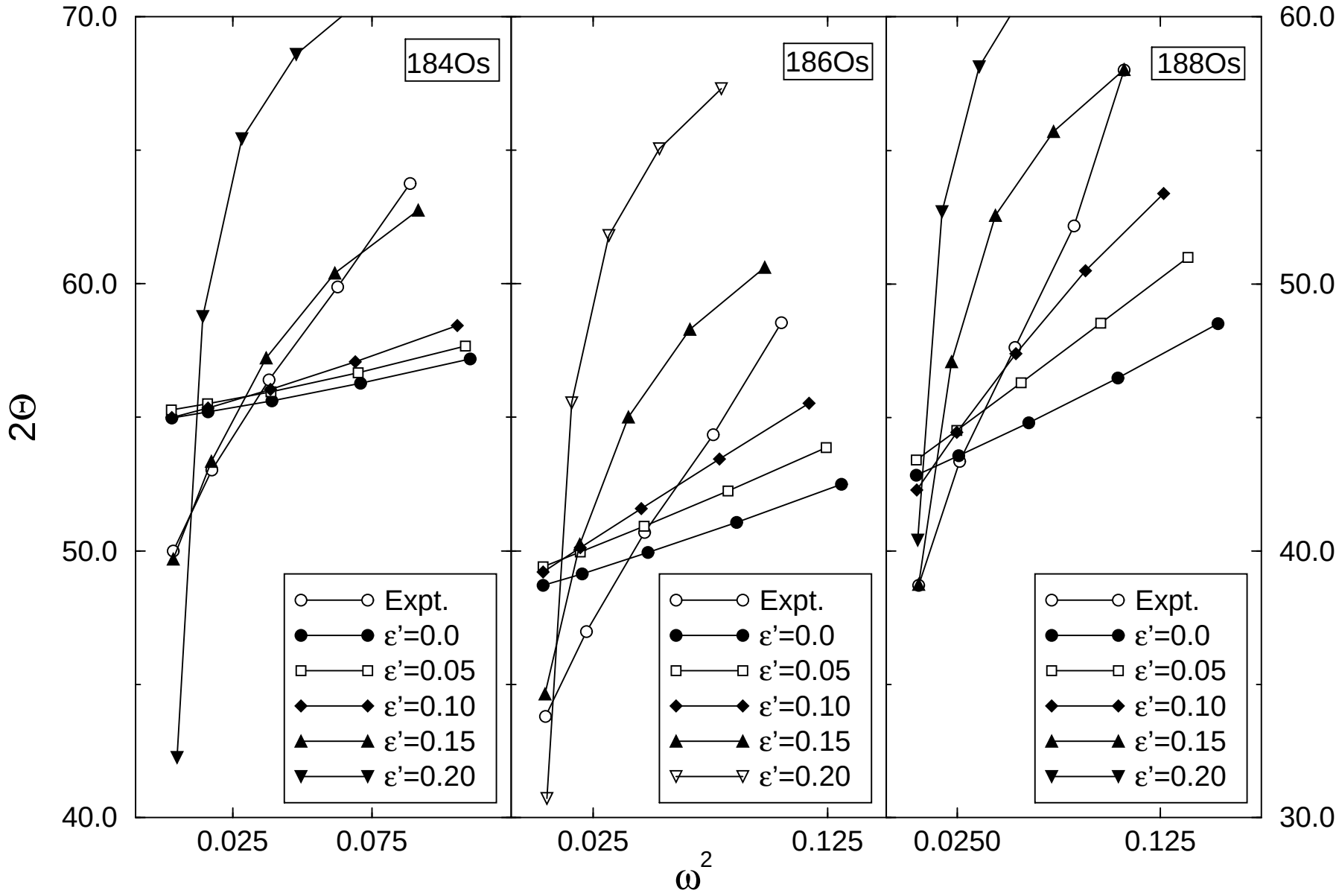
184Os
186Os
188Os
Expt.
ε'=0.0
ε'=0.05
ε'=0.10
ε'=0.15
ε'=0.20
2Θ
ω²
70.0
60.0
50.0
40.0
30.0
0.025
0.075
0.125
0.0250